

Faculty of Engineering National University of Colombia

National University of Colombia



PROJECT

Implementation, analysis, and qualitative evaluation of the Hodgkin-Huxley computational model as a general model for the action potential in neurons

Bioinformatics

Dr. Prof. [Emiliano Barreto Hernandez](#)

by

Carlos Andres Rios Rojas

Bogotá, Colombia

ID: 2020-1932265126

Group: 1

(Note: This document is a translation from the original Spanish text using Artificial Intelligence.)

Introduction	3
1.1. Problem Statement	3
1.2. Objectives	4
1.3. Methodology	4
1.4. Theoretical Framework	6
1.4.1. Ideal Spiking Neuron	6
1.4.2 Action Potential	7
1.4.3. Synapse	7
1.4.4. Nernst Potential	8
1.4.5. Resting Potential	10
1.4.6. Definition of the Hodgkin-Huxley Model	10
1.4.7. Dynamics of the Action Potential in the Hodgkin-Huxley Model	14
1.5. Computational Implementation	15
1.6. Analysis of Results	16
1.6. Comparison with Real Data	24
1.7. Conclusions	25

1. Introduction

1.1. Problem Statement

Following the work conducted by Santiago Ramón y Cajal, it became possible to characterize the composition of the nervous system for the first time, identifying nerve cells called "neurons" as the functional units, thus giving rise to the "neuron doctrine". The question that immediately followed this discovery was: "How do neurons interact with each other for the nervous system to function?".

Subsequently, the importance of the bioelectric phenomenon called "action potential" was determined. This is a brief electrical pulse that forms the basis of the mechanism by which a neuron is able to receive a stimulus from other neurons (called presynaptic neurons) via its dendrites and transmit it to other neurons (called postsynaptic neurons) through its axon. For this reason, to understand how neurons propagate these pulses and to study the underlying information, it is necessary to formulate a mathematical model that allows us to describe and quantitatively predict the occurrence of these phenomena in neurons. Such a model was first formulated in 1952 with the work of Alan Hodgkin and Andrew Huxley. Through experiments performed on tissue extracted from the giant axon of the squid, they inferred a mathematical model describing how the dynamic behavior of ion channels in the cell membrane is responsible for regulating the membrane potential.

In their work, they modeled the cell membrane as an electrical circuit where it was observed that the potential undergoes a sharp increase upon receiving an external current stimulus, corresponding to the neuron's action potential.

However, experimental methods are limited in deeply understanding how the variation of different model parameters affects its behavior. Therefore, experimentation through computational simulation becomes pertinent.

1.2. Objectives

General Objective To formulate, implement, and computationally analyze the Hodgkin-Huxley model to understand the dynamics of the action potential and evaluate its capacity to represent the electrical activity of different types of neurons.

Specific Objectives

- To formulate the Hodgkin-Huxley mathematical model and understand the biophysical principles that sustain it.
- To implement the Hodgkin-Huxley mathematical model in a computational environment.
- To simulate the behavior of the model under different levels of injected current to study the excitatory response.
- To evaluate the generality and limitations of the model by comparing computational simulations with real electrophysiological recordings of neurons from different nervous tissues and organisms.

1.3. Methodology

This work was developed through a computational and theoretical approach, based on the formulation and simulation of the Hodgkin-Huxley mathematical model for a single neuron.

The methodology is divided into the following stages:

- 1. Theoretical review of the Hodgkin-Huxley model:** A bibliographic review of the physiological and mathematical bases supporting the model was conducted to establish the necessary foundations for the subsequent development of the work.
- 2. Mathematical formulation of the Hodgkin-Huxley model:** Each part of the Hodgkin-Huxley model was constructed and justified, starting from the representation of the cell membrane as an electrical circuit to the formulation of the differential equations describing the model's behavior.
- 3. Computational Implementation:** The model was implemented using the Python programming language, utilizing auxiliary libraries for mathematical calculations and result display.
- 4. Model Simulation:** The model's response to different input current intensities was simulated to observe the generation of action potentials and their dependence on parameters.
- 5. Comparison with real data:** The model's response was simulated using parameters specific to neurons from mouse and human nervous tissues, comparing the behavior obtained with corresponding real electrophysiological results.
- 6. Analysis of results:** Data obtained from simulations were analyzed, identifying how parameter variation affects the model's behavior.
- 7. Conclusions:** Finally, the findings obtained from the simulations will be discussed, highlighting the utility of the Hodgkin-Huxley model as a computational tool for understanding neuronal bioelectric dynamics.

1.4. Theoretical Framework

1.4.1. Ideal Spiking Neuron

A typical neuron is functionally divided into three main parts: the dendrites, the soma, and the axon. Broadly speaking, dendrites fulfill the function of receiving signals from other neurons and transmitting them to the soma. The soma can be viewed as the central processing unit of the neuron. Here, signals received by the dendrites are processed non-linearly, where an output signal is generated if a specific threshold is exceeded. This output signal is transmitted to other neurons through the axon. The junction between two neurons is called a synapse, where the neuron sending the signal is called the presynaptic neuron and the one receiving the signal is called the postsynaptic neuron.

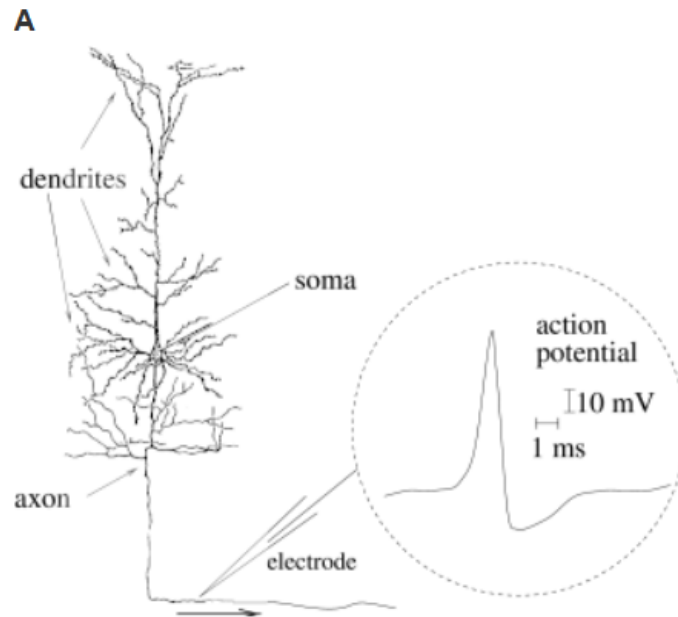


Figure 1: Illustration of a typical neuron. Taken from [2].

1.4.2 Action Potential

The signals transmitted by neurons consist of short electrical impulses called action potentials or spikes. These impulses have an amplitude of around 100 mV along with a typical duration of 1 to 2 ms. It is important to highlight that the shape of the pulses does not change as they propagate through the neuron's axon. A chain of action potentials emitted by a single neuron is called a spike train; that is, a sequence of stereotypical events occurring at regular or irregular intervals. As previously mentioned, because the shape of the spikes does not vary, the shape itself does not contain information; rather, it is the number of spikes and the time interval in which they occur that contains information.

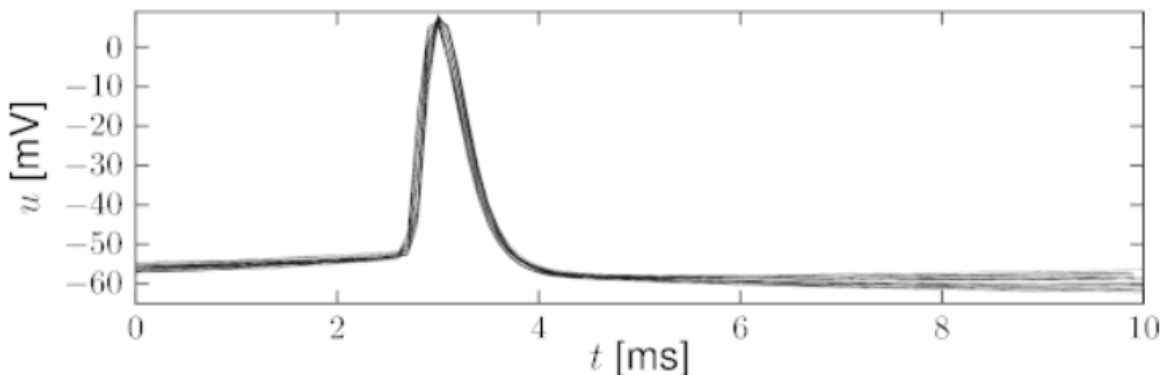


Figure 2: This graph shows the lack of variety in the shape of an isolated spike from a neuron. Taken from [2].

1.4.3. Synapse

The site where the axon of a presynaptic neuron makes contact with the dendrite (or soma) of a postsynaptic neuron is called a synapse. The most common type of synapse found in the vertebrate brain is the chemical synapse. In a chemical synapse, the axon terminal approaches the postsynaptic neuron without touching it, leaving a very small space between the cell

membranes of both neurons. This space is called the synaptic cleft. When an action potential reaches the synapse, it triggers a complex series of biochemical steps leading to the release of neurotransmitters from the presynaptic neuron's terminal into the synaptic cleft. These neurotransmitters are detected by specialized receptors on the postsynaptic neuron's membrane, leading to the opening of specific ion channels, which in turn causes an ion flux into the cell. This ion flux alters the membrane potential; therefore, the chemical signal is translated into an electrical response in the postsynaptic neuron. The response voltage of a postsynaptic neuron to a presynaptic spike is called the postsynaptic potential.

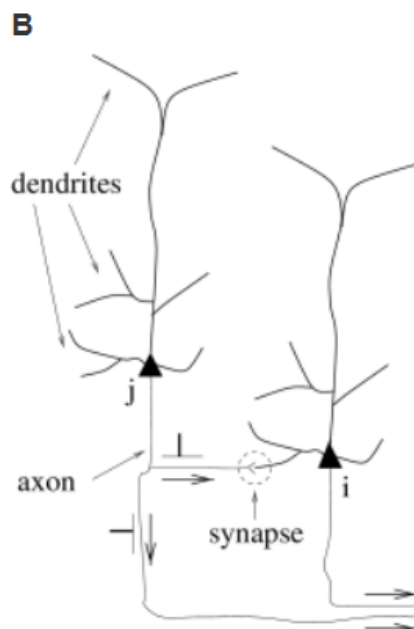


Figure 3: Illustration of a synapse between two typical neurons. Taken from [2].

1.4.4. Nernst Potential

The following derivation is taken from. Neurons are delimited by a membrane that separates the cell interior from the exterior. Ions exist both inside and outside the cell, and the ion concentration differs in both cases. From thermodynamics, the density of positive ions at a

specific position x within an electrostatic field is proportional to $\exp [-qu(x)/kT]$, where q is the ion charge, $u(x)$ is the potential energy at that position, k is the Boltzmann constant, and T is the temperature. Assuming the ion density at x is $n(x)$, and considering $q > 0$, the relationship between two positions x_1 and x_2 is given by:

$$\frac{n(x_1)}{n(x_2)} = \exp \left[-\frac{qu(x_1) - qu(x_2)}{kT} \right]$$

Thus, an electrical potential difference (a voltage) $\Delta u = u(x_1) - u(x_2)$ generates a difference in ion density at both positions. Since this is an equilibrium state, it is also concluded that a difference in ion proportion produces an electrical potential difference. Assuming that $n(x_1) = n_1$ y $n(x_2) = n_2$, and solving for Δu , we have

$$\Delta u = \frac{kT}{q} \ln \frac{n_2}{n_1}$$

This corresponds to the potential difference when the system is in equilibrium, which is called the Nernst potential.

The vital point here is to observe how a potential difference generates a gradient in the system's ion concentration.

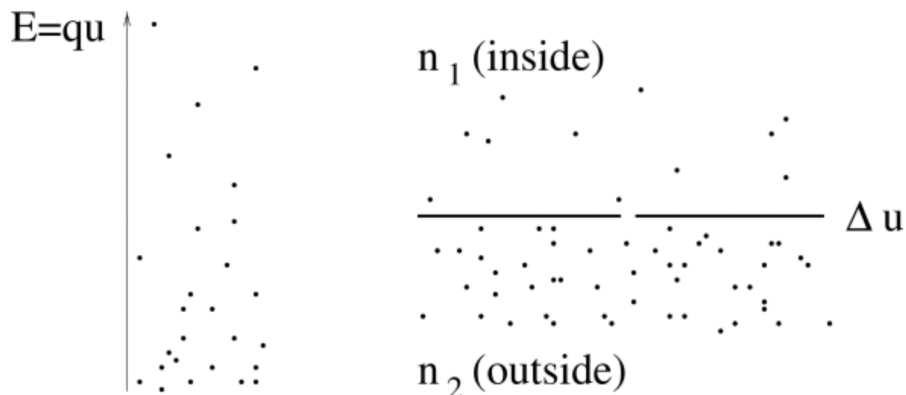


Figure 4: Illustration of Nernst potential. Taken from [5].

In the cell membrane, there are specialized proteins acting as gates for ions: ion channels (passive transport) and ion pumps (active transport). A Nernst potential for a single ion type (such as the sodium ion Na^+) can also be understood as a reversal potential, since the current (ion flow) through the membrane changes depending on the actual potential difference relative to the Nernst potential to maintain electrochemical equilibrium.

1.4.5. Resting Potential

The following derivation is taken from. In real cells, different types of ions contribute simultaneously to the membrane voltage. Experimentally, it was determined that the membrane resting potential is $u_{\text{rest}} \approx -65 \text{ mV}$. Considering that the Nernst potentials for sodium and potassium ions are approximately $E_{\text{Na}} \approx +67 \text{ mV}$ y $E_{\text{K}} \approx -83 \text{ mV}$ respectively, then $E_{\text{K}} < u_{\text{rest}} < E_{\text{Na}}$. This generates a constant flux in the membrane through ion channels to maintain this potential, where potassium ions exit while sodium ions enter. This flux is balanced and maintained thanks to the action of ion pumps. For this reason u_{rest} is determined by the dynamic equilibrium between the flux through ion channels (membrane permeability) and active ion transport (maintenance of concentration difference by ion pumps).

1.4.6. Definition of the Hodgkin-Huxley Model

La siguiente derivación se toma de [4]. The following derivation is taken from. The Hodgkin-Huxley model is based on experiments performed on the giant squid axon, where three distinct ion currents were found: sodium (Na^+), potassium (K^+), and a leak current (L) constituted mainly by Cl^- ions. It was also determined that specific channels (one for sodium

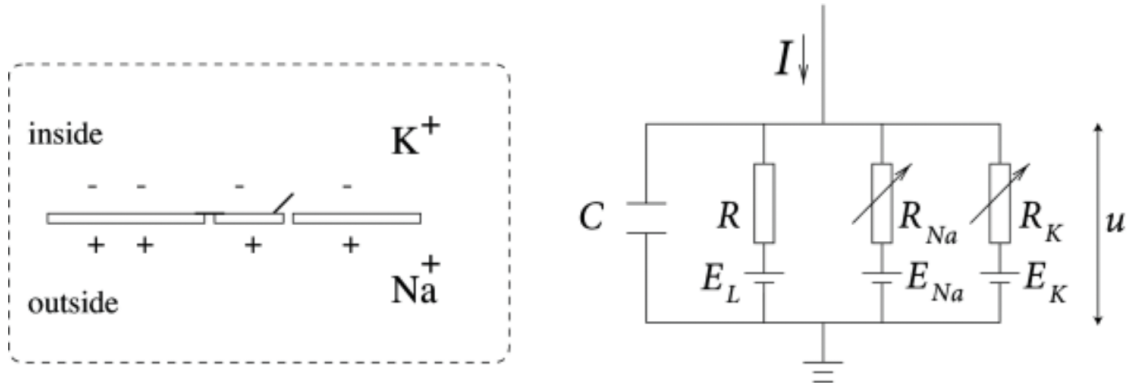


Figure 5: Schematic diagram of the Hodgkin-Huxley model. Taken from [4].

ion flow and another for potassium ion flow, i.e., no mixed channels) control the flow across the membrane, where these channels are voltage-dependent. The leak current occupies other types of channels not explicitly described by the model.

The model represents the cell membrane as a capacitor, such that when an external current I is applied to the cell, the membrane can charge or filter the current through ion channels. Each type of ion channel is represented as a resistor, where the non-specific channel corresponding to the leak current is represented as R , the sodium channel as R_{Na} , and the potassium channel as R_K . The latter two are variable, thus representing the dynamics in which these channels can close or open. The action of ion pumps maintains a difference in ion concentrations inside and outside the cell, generating a Nernst potential for each ion type, represented by a battery. Thus, there are three distinct batteries for the leak, sodium, and potassium channels respectively: E_L , E_{Na} y E_K .

From the above, the total current is:

$$I(t) = I_C(t) + \sum_k I_k(t)$$

From the definition of capacitance $C = q/u$, where q is charge and u is the voltage across the capacitor, it is deduced that $I_C = C du/dt$, thus:

$$C \frac{du}{dt} = - \sum_k I_k + I(t)$$

The model describes the three channel types considered initially via their respective conductances. For the leak channel, a voltage-independent conductance $g_L = 1/R$, is used, and by Ohm's law, $I_L = g_L(u - E_L)$. For the other two channel types, the conductance depends on voltage and time to represent their ability to close or open. The model introduces three variables taking values from 0 to 1 called gating variables: m , n and h where m and n are activation variables and h is an inactivation variable. With this, the effective conductances for sodium and potassium channels are defined respectively as:

$1/R_{Na} = g_{Na} m^3 h$ y $1/R_K = g_K n^4$, with g_{Na} and g_K being the corresponding maximum conductances. Thus, we have:

$$\sum_k I_k = g_{Na} m^3 h (u - E_{Na}) + g_K n^4 (u - E_K) + g_L (u - E_L) .$$

The three gating variables evolve according to differential equations of the form

$$\dot{x} = - \frac{1}{\tau_x(u)} [x - x_0(u)]$$

where $\dot{x} = dx/dt$ and x corresponds to the gating variable m , n or h . These equations are interpreted as follows: for a fixed voltage u , the variable x approaches the target value $x_0(u)$ with a time constant $\tau_x(u)$. The curves corresponding to $x_0(u)$ and $\tau_x(u)$ for each gating variable were found experimentally and are shown in Figure 6. It should be clarified that in the original model, the system of equations determining gating variable behavior is described in terms of voltage-dependent transition rates α and β as

$$\dot{x} = \alpha_x(u) (1 - x) - \beta_x(u) x$$

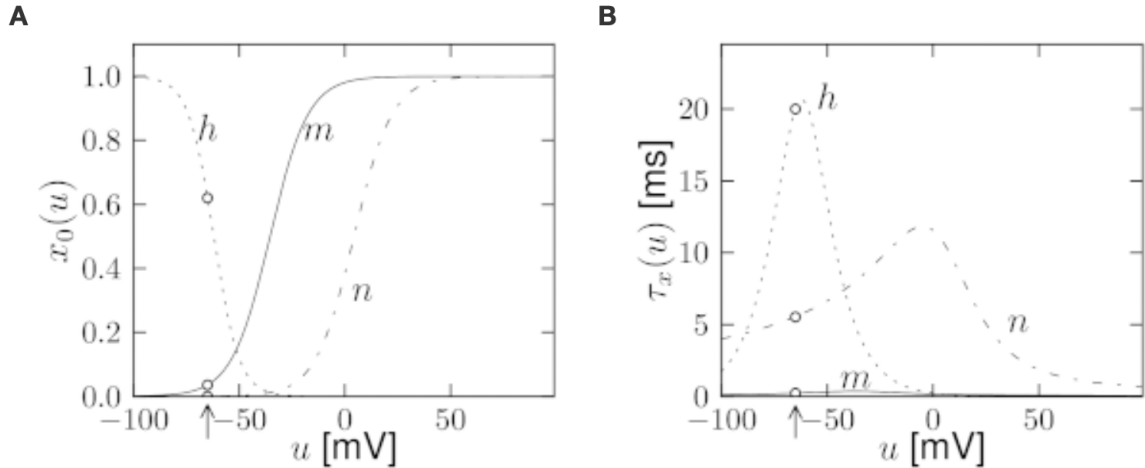


Figure 6. Graphs of (A) $x_0(u)$ and (B) $\tau_x(u)$ for the three gating variables m, n and h . Taken from [4].

which is equivalent to the previously presented system. The asymptotic value $x_0(u)$ and the time constant $\tau_x(u)$ are found via the transformations

$$x_0(u) = \frac{\alpha_x(u)}{\alpha_x(u) + \beta_x(u)},$$

$$\tau_x(u) = \frac{1}{\alpha_x(u) + \beta_x(u)}.$$

The parameters adjusted for the simulation of a pyramidal neuron of the cerebral cortex are presented in the following tables:

x	E_x [mV]	g_x [mS/cm ²]
Na	55	40
K	-77	35
L	-65	0.3

Table 1. Nernst potential parameters and ion channel conductance. Data taken from [4].

x	$\alpha_x (u / \text{mV}) [\text{ms}^{-1}]$	$\beta_x (u / \text{mV}) [\text{ms}^{-1}]$
n	$0.02 (u - 25) / [1 - e^{-(u-25)/9}]$	$-0.002 (u - 25) / [1 - e^{(u-25)/9}]$
m	$0.182 (u + 35) / [1 - e^{-(u+35)/9}]$	$-0.124 (u + 35) / [1 - e^{(u+35)/9}]$
h	$0.25 e^{-(u+90)/12}$	$0.25 e^{(u+62)/6} / e^{(u+90)/12}$

Table 2. Gating variable parameters. Data taken from [4].

Similarly, the membrane capacitance value is experimentally obtained as $C = 1\mu\text{F}/\text{cm}^2$.

1.4.7. Dynamics of the Action Potential in the Hodgkin-Huxley Model

The following derivation is taken from [4]. From the equations describing the gating variables behavior, it is observed that m_0 and n_0 grow with u while h_0 decreases. This dynamics increases sodium channel conductance, further increasing membrane voltage, which in turn increases conductance again. This feedback process initiates the action potential upon exceeding a certain threshold. However, this explosive increase stops as it approaches the sodium current reversal potential E_{Na} .

As seen in figure 6, τ_h is always greater than τ_m , so h take much longer to reach their target value than m . Thus, for high values of u sodium channels slowly inactivate (close). In a similar time period, the potassium current establishes itself, and being an outward flow from the cell, it causes the membrane voltage to decrease. The joint action of sodium and potassium currents produces a short action potential followed by a negative overshoot prolonged in time called the after-hyperpolarization potential. This period of membrane voltage negativity is caused by the slowness of h to return to its initial value, thus slowing the reactivation of sodium channels.

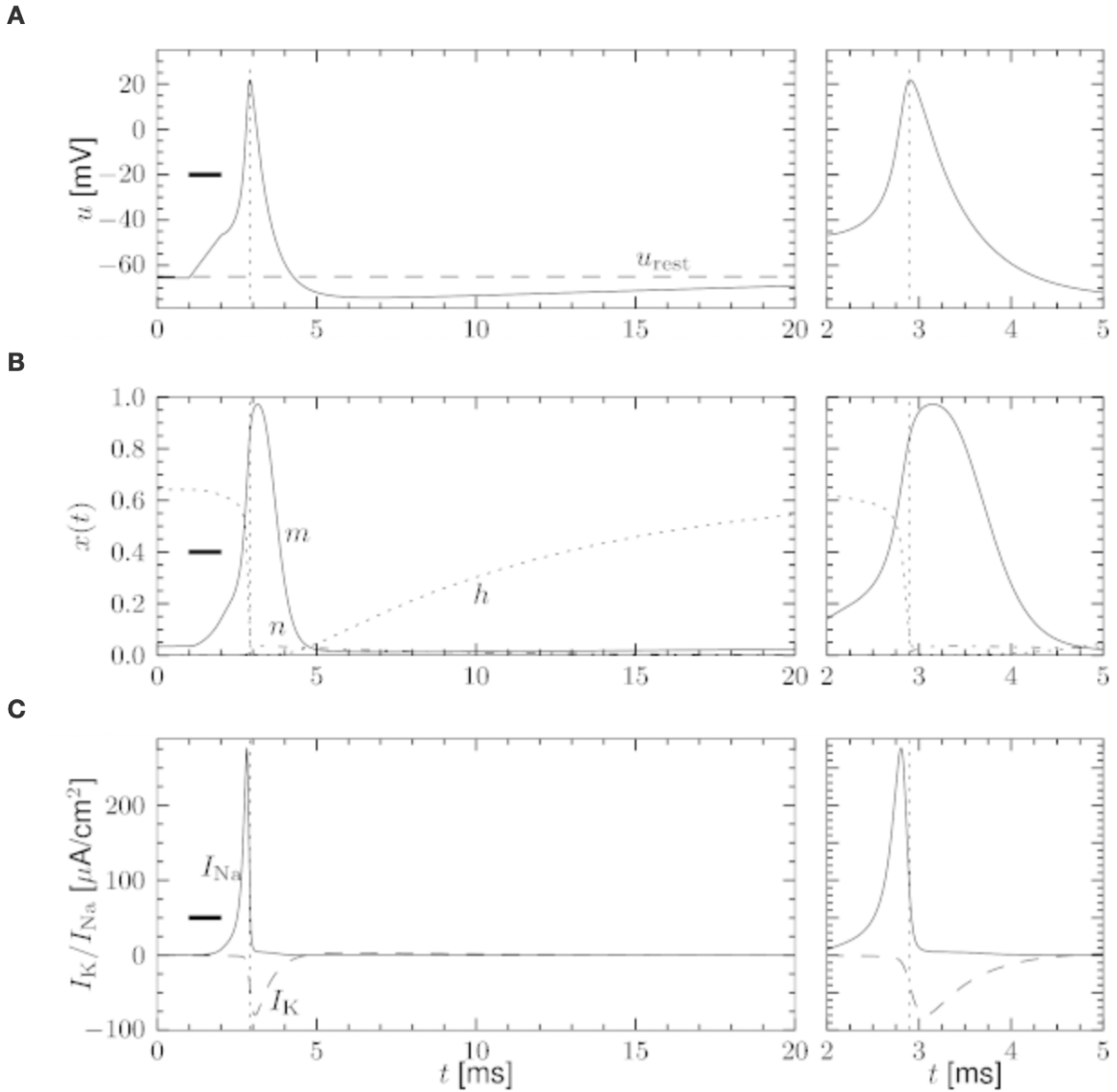


Figure 7. Graphs describing the general dynamics of the action potential in the model.

Taken from [4].

1.5. Computational Implementation

The model is implemented in the Python programming language, using only two libraries (Numpy and Matplotlib).

The program consists of a set of functions constituting the simulation. The heart of the simulation is the implementation of Runge-Kutta 4 to solve the coupled system of differential equations. The program allows simulation with different parameter sets via the model

simulation function parameters, as well as the construction of a dictionary containing parameters specific to the cell intended for simulation. The program also receives a function as input current, thus allowing simulations where current varies with time. Results are displayed as graphs describing the evolution of membrane potential, gating variables, and input current throughout the simulation. The program is attached as an annex to this work.

1.6. Analysis of Results

The model simulation is performed using parameters shown in Table 1 and Table 2 corresponding to a pyramidal neuron of the cerebral cortex. The simulated time period is 140 ms, where in the first 120 ms a constant current increasing from 0 μA is applied. $dt = 1$ ms is used.

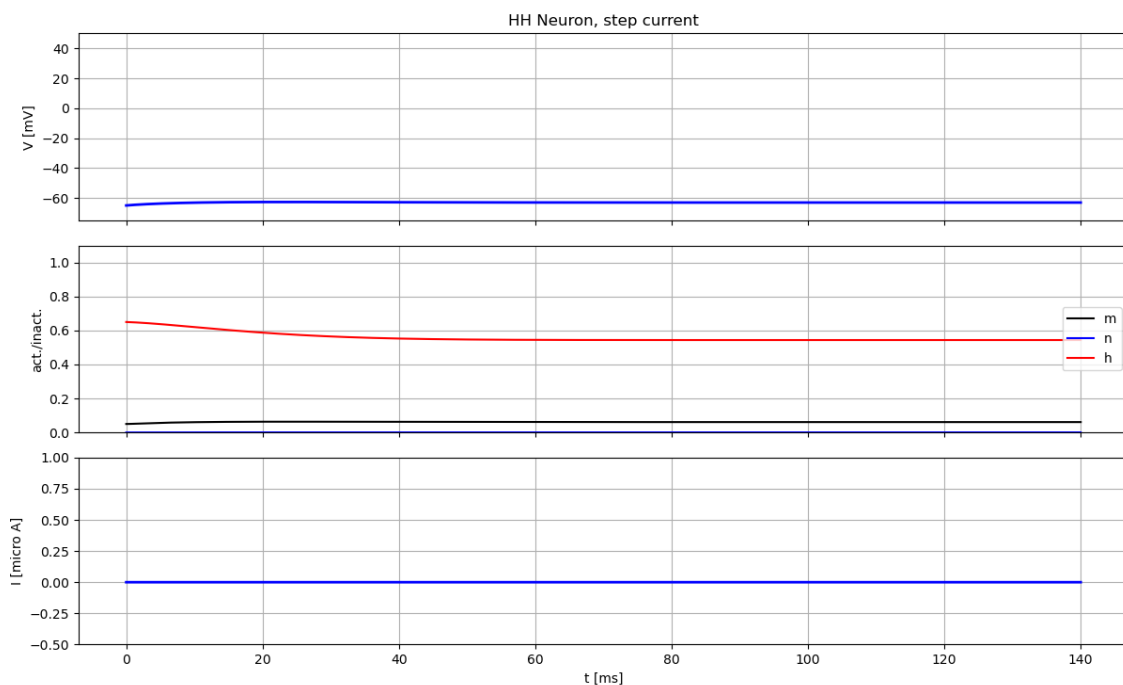


Figure 8. Results for 0.0 μA . Own authorship.

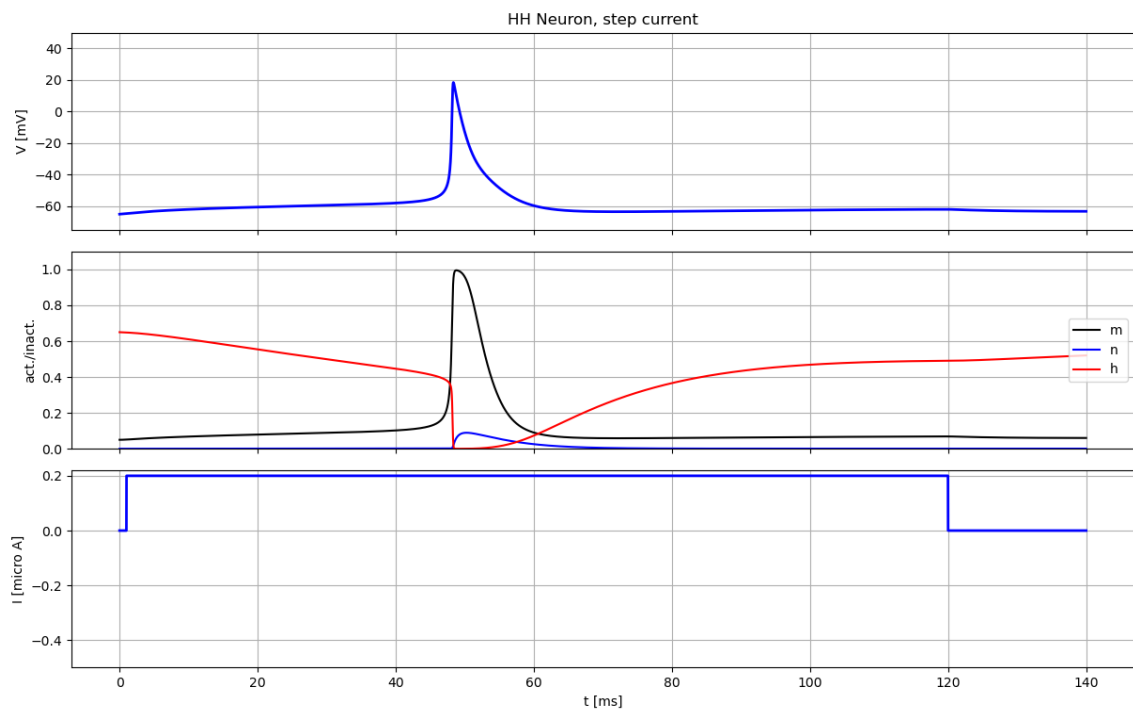


Figure 9. Results for $0.2 \mu\text{A}$. Own authorship.

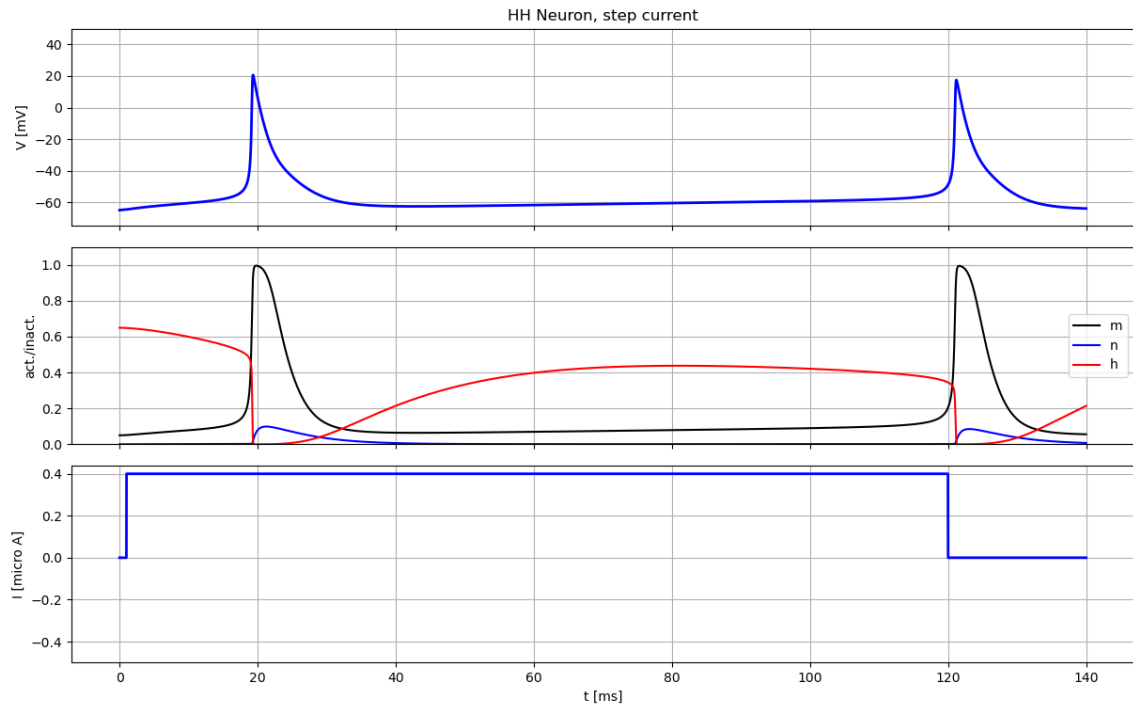


Figure 10. Results for $0.4 \mu\text{A}$. Own authorship.

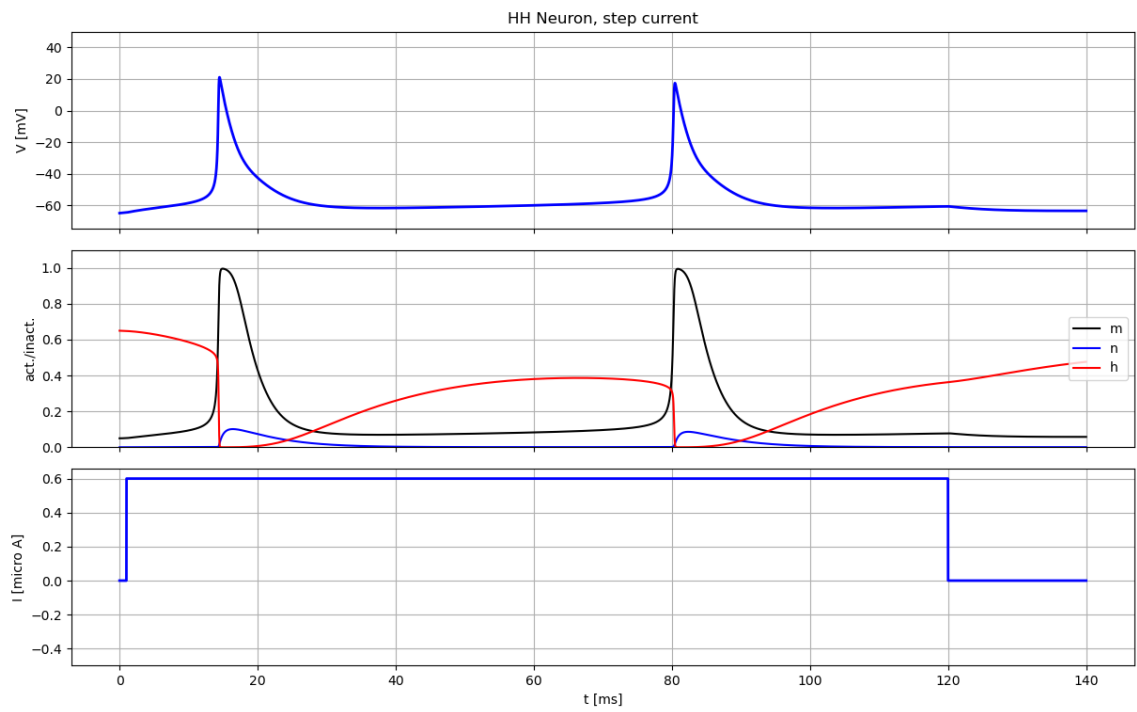


Figure 11. Results for $0.6 \mu\text{A}$. Own authorship.

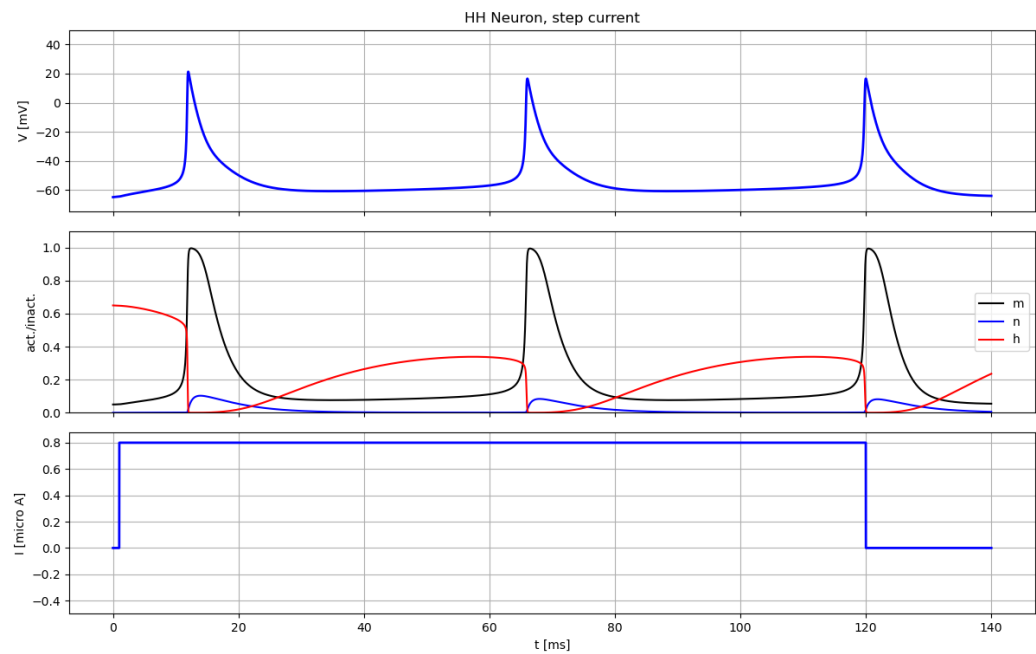


Figure 12. Results for $0.8 \mu\text{A}$. Own authorship.

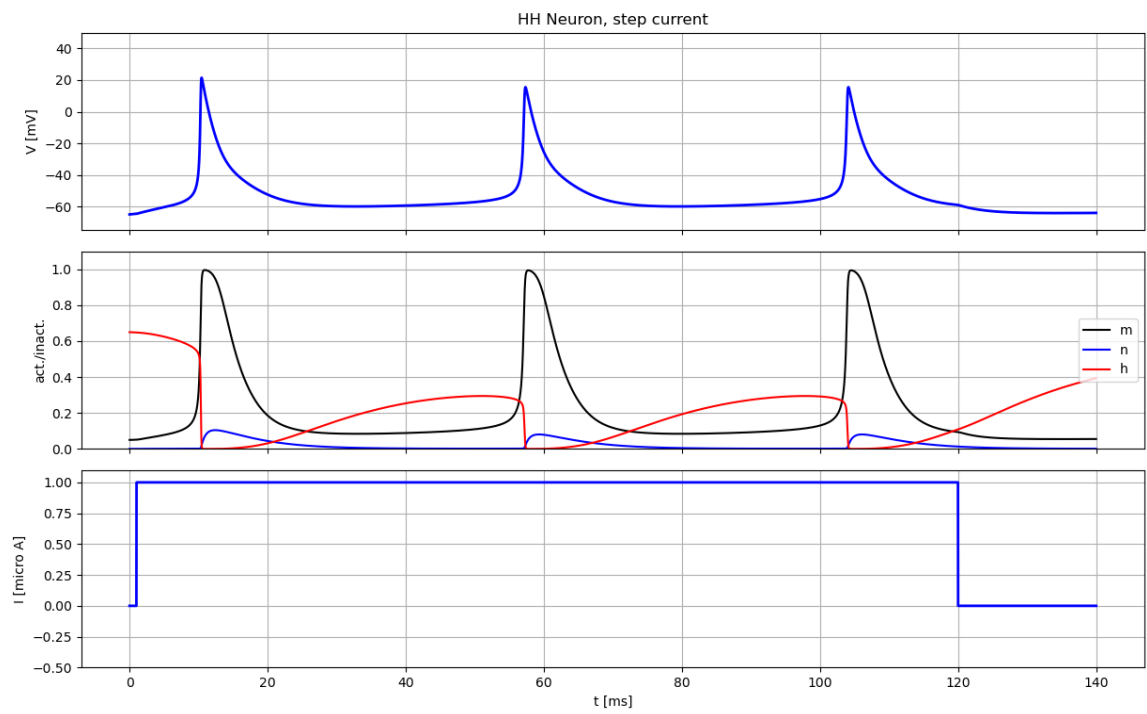


Figure 13. Results for $1.0 \mu A$. Own authorship.

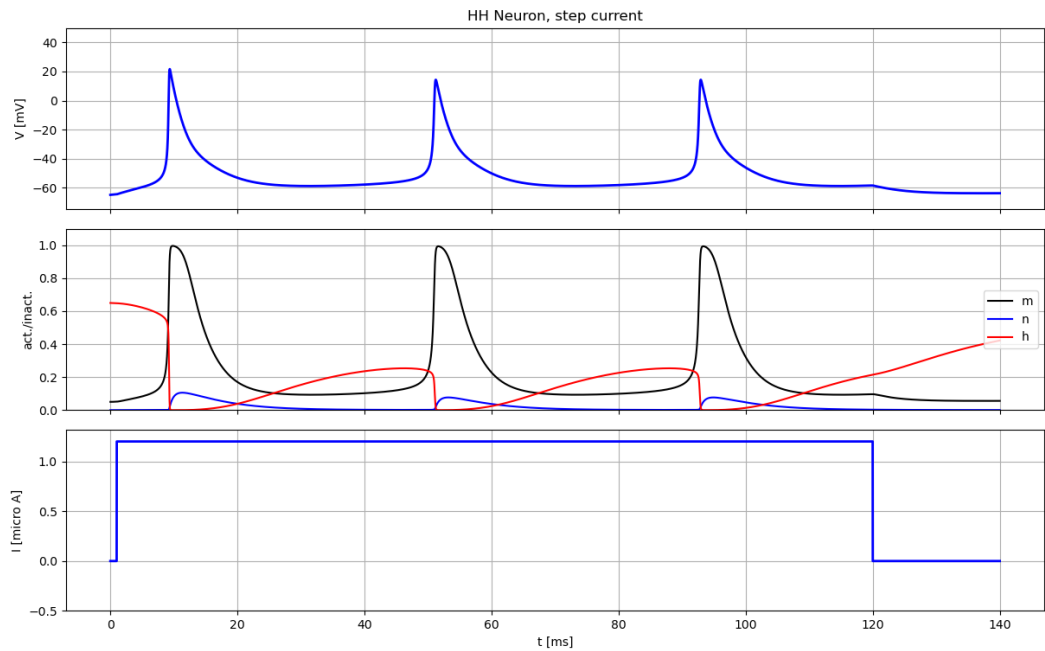


Figure 14. Results for $1.2 \mu A$. Own authorship.

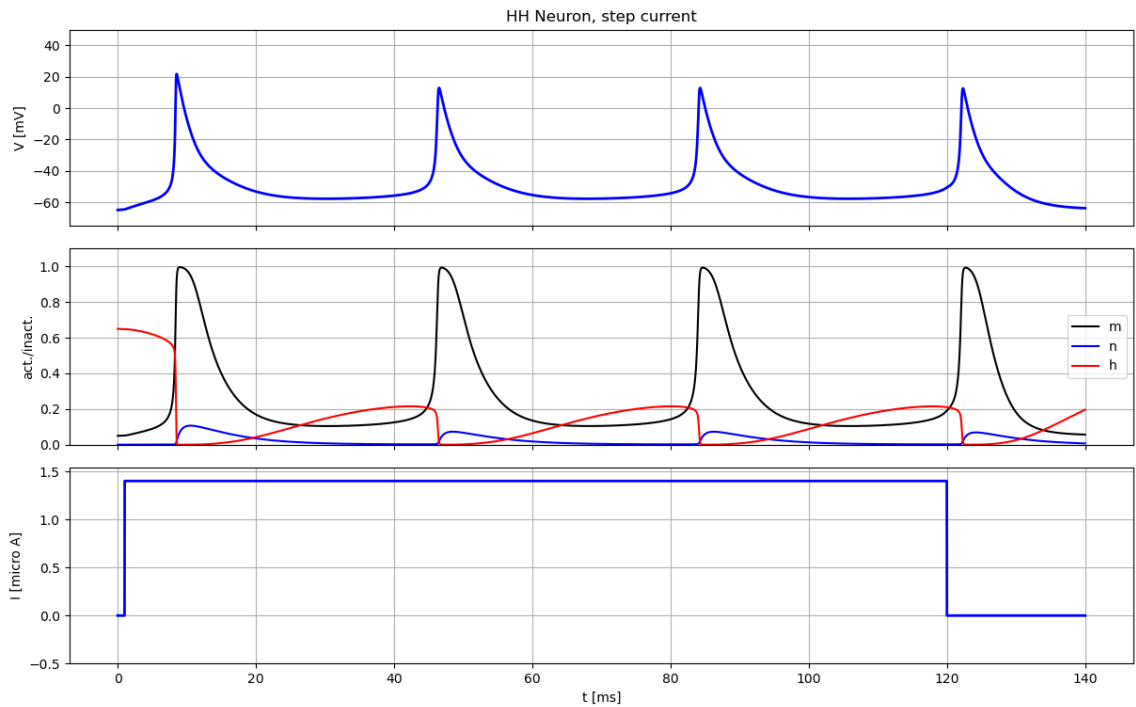


Figure 15. Results for $1.4 \mu\text{A}$. Own authorship.

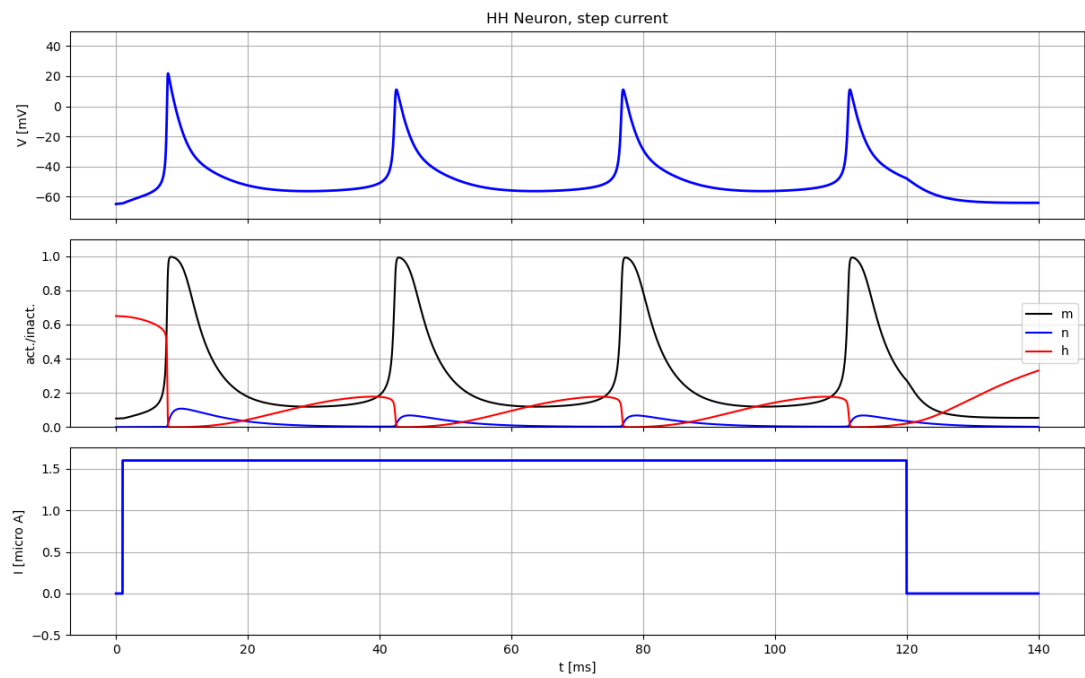


Figure 16. Results for $1.6 \mu\text{A}$. Own authorship.

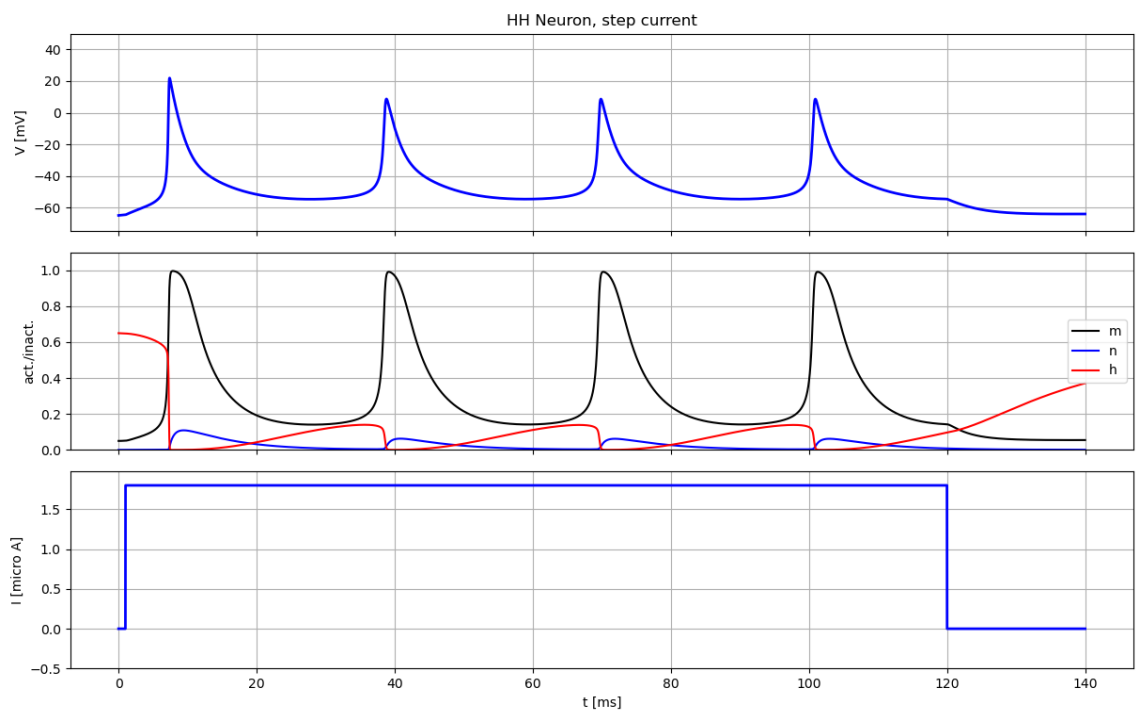


Figure 17. Results for $1.8 \mu\text{A}$. Own authorship.

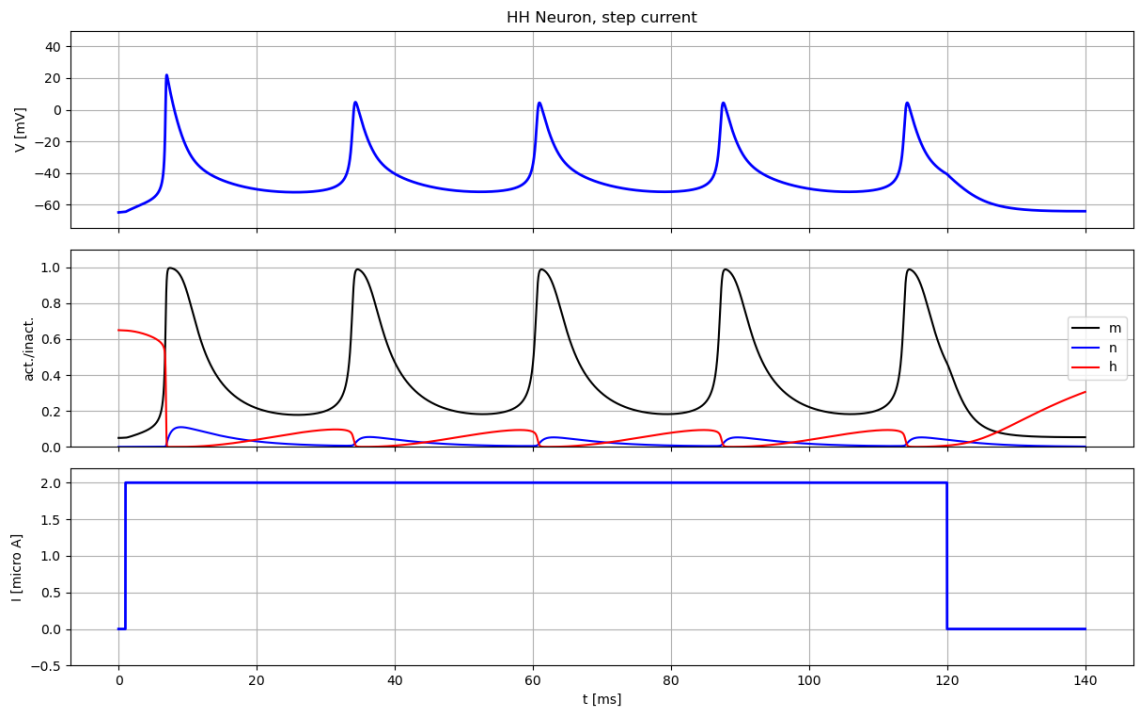


Figure 18. Results for $2.0 \mu\text{A}$. Own authorship.

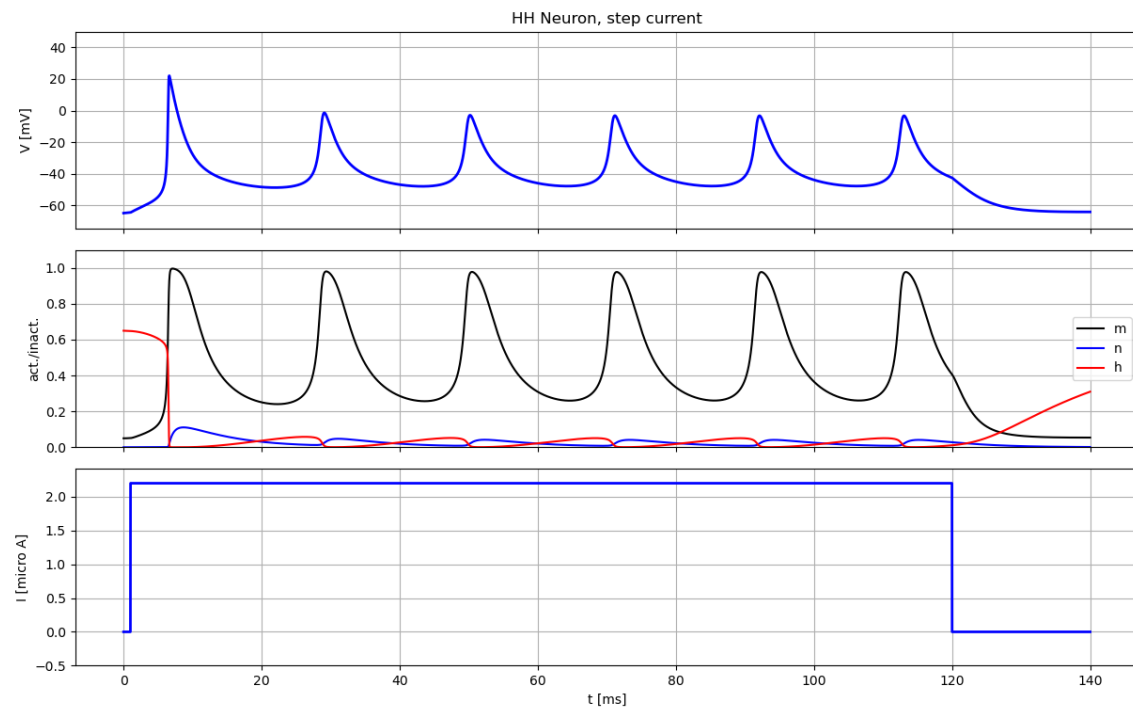


Figure 19. Results for $2.2 \mu\text{A}$. Own authorship.

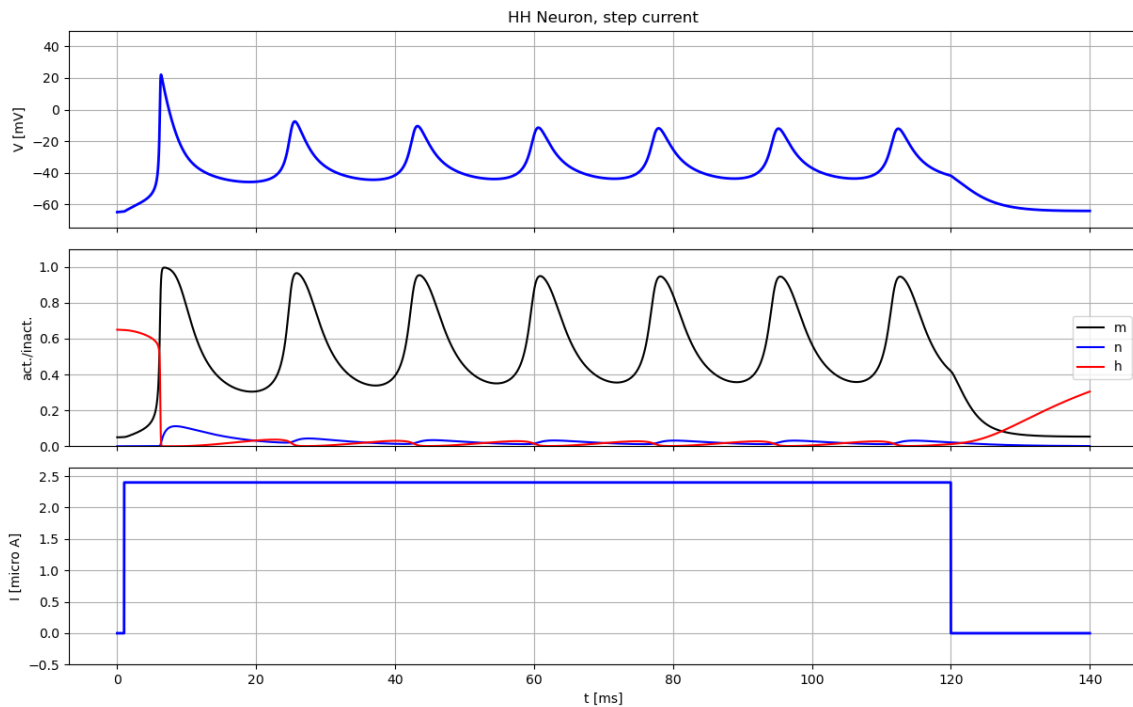


Figure 20. Results for $2.4 \mu\text{A}$. Own authorship.

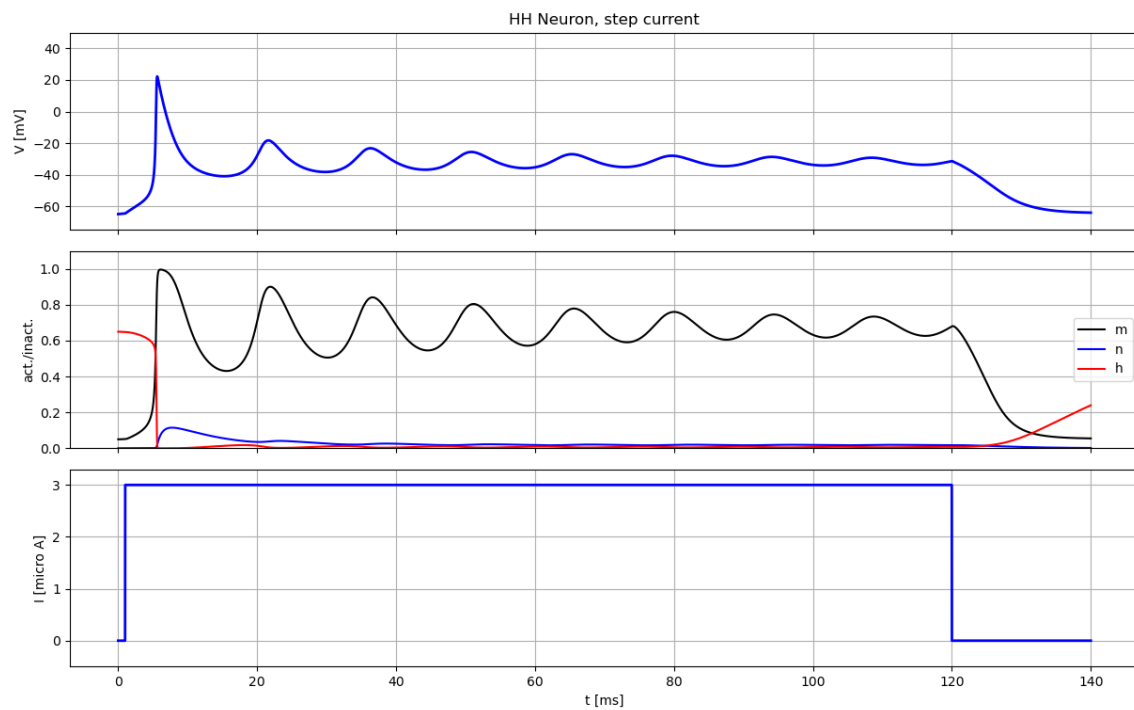


Figure 21. Results for $3.0 \mu A$. Own authorship.

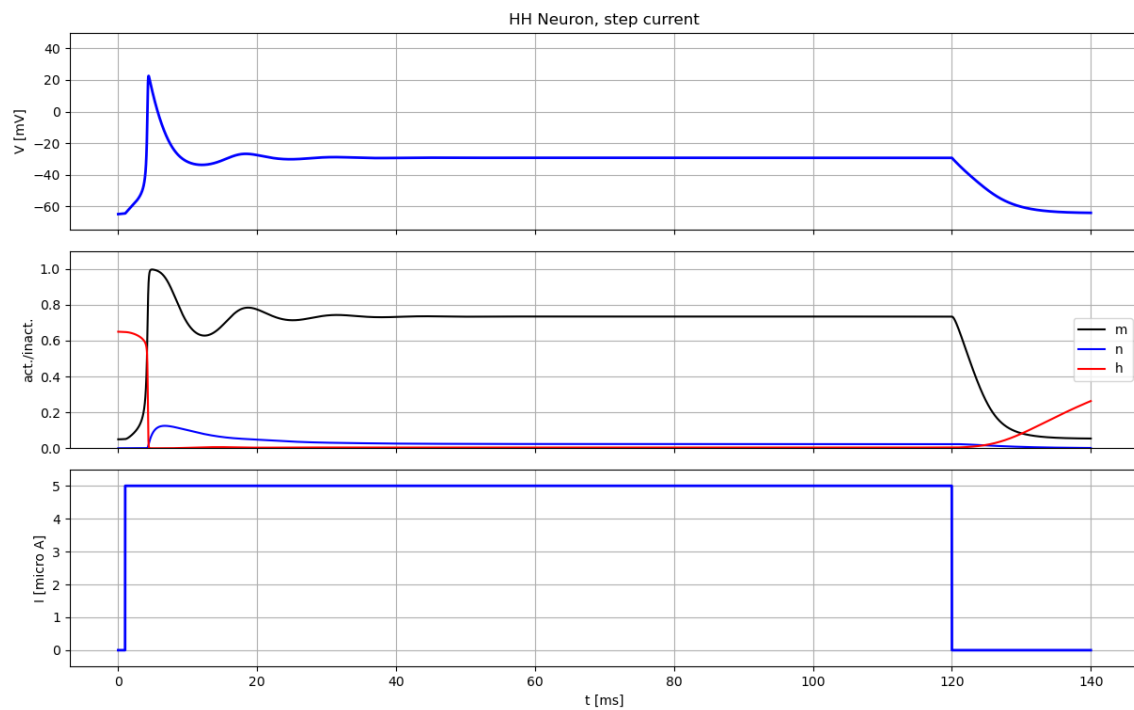


Figure 22. Results for $5.0 \mu A$. Own authorship.

The results indicate that the implementation correctly simulates the expected behavior observed in Figure 7. Initially, it is observed how, in the absence of external current, the model maintains its equilibrium potential (Figure 8). An increase in firing frequency is observed as current increases in the $0.0 \mu A$ - $2.0 \mu A$ range (Figure 9 to Figure 18). From $2.0 \mu A$, an increase in frequency is still observed alongside a decrease in the amplitude of each action potential (Figure 19 to Figure 21).

Finally, in Figure 22, we see how the initial spike presents itself and subsequently the model maintains a voltage higher than its equilibrium voltage of around -35 V. The previous behavior is explained because as current increases, the model's repolarization period decreases, increasing firing frequency. However, when the input current is very high, given the specific parameters of the cell being simulated, the ion channel dynamics fail to effectively repolarize the cell, causing this blockade observed in the final simulation results.

1.6. Comparison with Real Data

To test the generality of the Hodgkin-Huxley model, literature regarding the Plateau potential, a type of action potential found in multiple neuron types, is reviewed. From information found in [7], it is observed that for the description of this potential type in *Aplysia californica* neurons, the inclusion of additional parameters not included in the original model is fundamental.

As can be seen in Figure 23, the model used in [7] includes different ion channels (such as CaR and CaL) such that the original Hodgkin-Huxley model would be ineffective for simulating this neuron's functioning, and more specifically, for reproducing the generation of the Plateau potential observed in this type of neurons. This is sufficient to demonstrate that

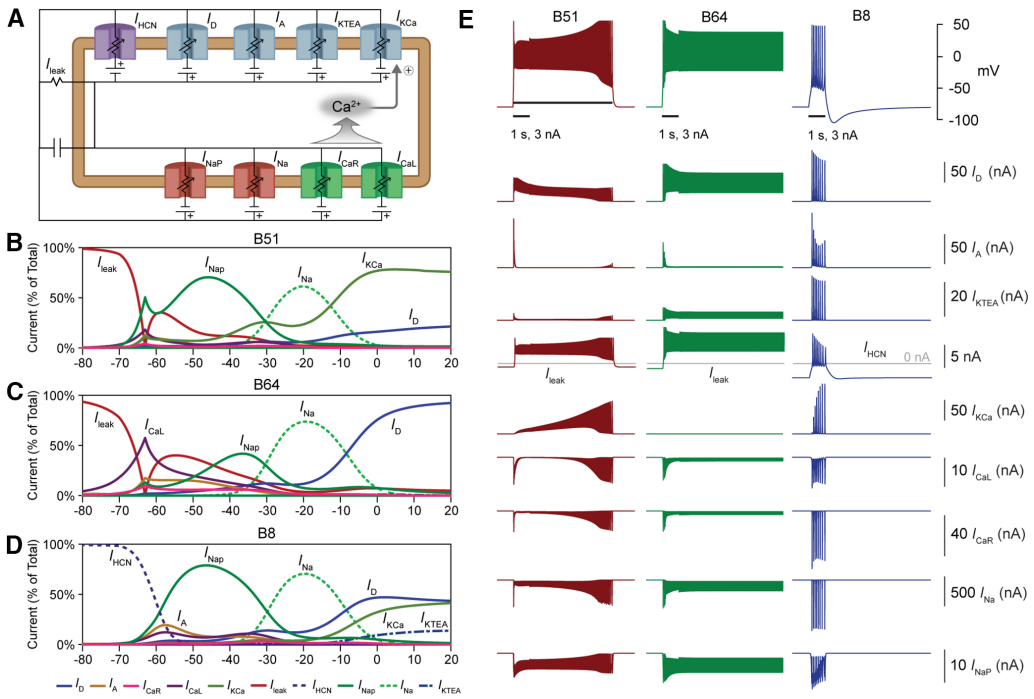


Figure 23. Simulation results and model diagram. Taken from [7].

the implemented model is not general and requires extensions and data adjustment to be used properly.

1.7. Conclusions

The implemented Hodgkin-Huxley model accurately reproduced the fundamental dynamics of the action potential for parameters characteristic of a pyramidal neuron of the cerebral cortex. The classic phenomena described by the original model were observed: firing threshold, depolarization phase dominated by sodium current, repolarization mediated by potassium, and the hyperpolarizing afterpotential.

Likewise, the simulation showed the progressive increase in firing frequency against increased injected current, as well as depolarization block at elevated currents, behavior consistent with experimental reports.

The comparison with real data allowed establishing that, although the Hodgkin-Huxley model constitutes a powerful tool for describing the basic electrophysiology of a typical neuron, its generalization capacity is limited. In particular, the appearance of phenomena like Plateau potentials in *Aplysia* neurons requires the inclusion of additional channels not contemplated in the original model, such as L-type and R-type calcium-dependent currents. This demonstrates that the model must be extended or re-parameterized to adequately capture the functional diversity of different neuronal types.

Collectively, this work evidences both the utility and limitations of the Hodgkin-Huxley model. Its mathematical structure allows for a quantitative understanding of the biophysical mechanisms generating the action potential, but also shows that the complexity of real neuronal activity demands more detailed models when studying specialized cells or non-standard dynamic behaviors. With this, the project fulfills the objective of analyzing the model from a computational perspective and critically reflecting on its applicability in modern neuroscience.

References

1. Mishqat I. *The Neuron Doctrine (1860-1895)*. Embryo Project Encyclopedia [Internet]. Arizona State University; 15 junio 2017 [citado 2025 Nov 22]. Disponible en: <https://embryo.asu.edu/pages/neuron-doctrine-1860-1895>
2. Gerstner W, Kistler WM, Naud R, Paninski L. *1.1 Elements of Neuronal Systems*. In: *Neuronal Dynamics – From Single Neurons to Networks and Models of Cognition* [Internet]. Lausanne: EPFL; c2014 [cited 2025 Nov 22]. Available from: <https://neuronaldynamics.epfl.ch/online/Ch1.S1.html>
3. Schwiening CJ. A brief historical perspective: Hodgkin and Huxley. *J Physiol*. 2012 Jun 1;590(11):2571-5. doi:10.1113/jphysiol.2012.230458. PMID: 22787170. PMCID: PMC3424716.
4. Gerstner W, Kistler WM, Naud R, Paninski L. *2.2 Hodgkin-Huxley Model*. In: *Neuronal Dynamics – From Single Neurons to Networks and Models of Cognition* [Internet]. Lausanne: EPFL; c2014 [cited 2025 Nov 22]. Available from: <https://neuronaldynamics.epfl.ch/online/Ch2.S2.html>
5. Gerstner W, Kistler WM, Naud R, Paninski L. *2.1 Membrane Conductances and Channel Types*. In: *Neuronal Dynamics – From Single Neurons to Networks and Models of Cognition* [Internet]. Lausanne: EPFL; c2014 [citado 2025 Nov 22]. Disponible en: <https://neuronaldynamics.epfl.ch/online/Ch2.S1.html>
6. Hodgkin AL, Huxley AF. A quantitative description of membrane current and its application to conduction and excitation in nerve. *The Journal of Physiology*. 1952;117(4):500–544. doi:10.1113/jphysiol.1952.sp004764. PMCID: PMC1392413.
7. Neveu CL, Smolen P, Baxter DA, Byrne JH. Voltage- and calcium-gated membrane currents tune the plateau potential properties of multiple neuron types. *J Neurosci*.

2023 Nov 8;43(45):7601-7615. doi:10.1523/JNEUROSCI.0789-23.2023. PMCID:
PMC10634553.